Finite element analysis of pitting corrosion on mechanical behavior of E690 steel panel

Ming Liu

Center for Advancing Materials Performance from the Nanoscale (CAMP-Nano), State Key Laboratory for Mechanical Behavior of Materials, Xi'an Jiaotong University, Xi'an, China and State Key Laboratory for Strength and Vibration of Mechanical Structures, Xi'an Jiaotong University, Xi'an, China

Abstract

Purpose – The purpose of this study is to analysis the pitting corrosion on the mechanical behavior of E690 high-strength steel sandwich panel. The pitting corrosion depth and degree of pitting (DOP) damage were used to evaluate the mechanical behaviors such as peak load and specific energy absorption of E690 panel.

Design/methodology/approach – The mechanical behavior of quasi-static compression, low-speed impact and three-point bending of E690 panel after pitting corrosion was simulated by ABAQUS nonlinear finite element method.

Findings – The quasi-static compression and low-speed impact mechanical properties can be greatly reduced by the pitting corrosion of the panel core, the pitting corrosion of the outer panel shows no obvious effect. The mechanical properties decrease with the increase of the pitting corrosion depth and DOP, and the influence of DOP is greater than that of pitting corrosion depth. The DOP of outer panel has less effect on mechanical properties of three-point bending compared with that of the core. Therefore, the pitting corrosion in the core of panel should be strictly controlled to prevent adverse effects on the mechanical properties of the structure.

Originality/value – To make up for the deficiency of the research on the corrosion behavior of high-strength steel sandwich panel structure, this paper chose E690 high-strength steel panel as the research object, and nonlinear finite element method was adopted to simulate the influence of pitting corrosion coverage area and pitting depth on its mechanical property degradation. The quasi-static compression, low-speed impact and three-point bending mechanical properties of panel with various DOPs and pitting depths were systematic studied.

Keywords E690, Pitting corrosion, Mechanical behavior, Peak load, Simulation

Paper type Research paper

1. Introduction

Lightweight and multifunctional materials and structures have become the mainstream design of offshore engineering structures (Rabiee and Ghasemnejad, 2019; Kwon, 2019; Deifalla, 2020; Kalinin *et al.*, 2020). As a typical periodic lattice structure, corrugated metal sandwich panel has been widely used in engineering because of its advantages of simple preparation process, high stiffness and lightweight. Previous studies focused more on mechanical properties, design and manufacturing processes (Panda and Jagadeesha, 2021; Wang *et al.*, 2020; Deifalla, 2020; Bai *et al.*, 2019). However, it is necessary to study the mechanical behavior of panel in corrosive environment because malignant damage accidents are inevitable. There have been systematic studies on the failure behavior of high-strength steel in various corrosive environments (Liu *et al.*, 2017; Han *et al.*, 2019; Liu *et al.*, 2016; Liu *et al.*, 2019a, 2019b), but few reports are focusing on the mechanical behavior of high-strength steel panel in such environments.

We have studied the mechanical behavior of E690 high-strength steel panel after uniform corrosion by nonlinear finite element simulation (Liu, 2021). The results show that the outer panel corrosion has the least effect on the mechanical properties, the inner panel and core corrosion could greatly reduce its mechanical properties. Because of countless welding surfaces, this kind of panel may also have various types of defects in the manufacturing process. In particular stress state and corrosion environment, it will further develop and form more dangerous corrosion defects, and the influence of surface pitting on overall performance have been widely concerned (Said *et al.*, 2015; Chiodo and Ruggieri, 2009; Caleyo *et al.*, 2009). The probability distribution of pitting depth and corrosion rate, the growth model of pitting corrosion and pit-to-stress corrosion cracking have been widely reported. A variety of evaluation methods for pitting corrosion defects were also developed (Turnbull *et al.*, 2006; Anghel, 2009).

To make up for the deficiency of the research on the corrosion behavior of high-strength steel sandwich panel structure, this paper chose E690 high-strength steel panel as the research object, and nonlinear finite element method was adopted to simulate the influence of pitting corrosion coverage area

The current issue and full text archive of this journal is available on Emerald Insight at: **https://www.emerald.com/insight/0003-5599.htm**

Anti-Corrosion Methods and Materials
69/4 (2022) 351–361

[DOI 10.1108/ACMM-11-2021-2571]

The authors gratefully acknowledge the financial supports from the National Natural Science Foundation of China (No. 51801149) and the China State Key Laboratory for Mechanical Structure Strength and Vibration Open-end Foundation (No. SV2019–KF–10).

Conflicts of interest: The author declares no conflict of interest.

Received 10 December 2021
Revised 10 January 2022
Accepted 12 January 2022

area and pitting depth on its mechanical property degradation. The quasi-static compression, low-speed impact and three-point bending mechanical properties of panel with various degrees of pitting (DOPs) and pitting depths were systematic studied.

2. Details on the finite element model

2.1 Material and structure

In the present work, E690 high-strength steel was used for simulation (Zhao *et al.*, 2019). The tensile stress and the yield stress are 799 and 739 MPa, respectively.

The panel used in this study shown in Figure 1 refers to Yan *et al.* (2013), the inclination angle α is 45°, the thickness of upper, bottom and core t is 2 mm, the height of core body H is 23 mm and the sample width is 20 mm. The relative density of the panel can be calculated by the following formula (Yan *et al.*, 2013):

$$\overline{\rho} = \frac{t/H}{t/H + \cos\alpha} \tag{1}$$

2.2 Corrosion mode

Pitting is localized corrosion in the form of deep holes, each pitting has its own unique shape and depth. As for a common method, instead of modeling a single pit body, a group of pits body damage adjacent to each other is modeled by applying rectangles or circles (Chen *et al.*, 2018; Fu *et al.*, 2018; Saad-Eldeen *et al.*, 2013; Nakai *et al.*, 2006). Generally, the DOP damage is defined as the ratio of the corrosion area to the entire area (Rahbar-Ranji *et al.*, 2015):

$$\mathrm{DOP} = \frac{1}{ab}\sum_{i=1}^{n} A_{pi} \times 100(\%) \tag{2}$$

where A_{pi} is the area of each pit, n is the pits number and a and b are the length and width dimensions of the plate, respectively.

In this paper, the base pitting corrosion model is 2 mm × 2 mm cuboid with different depths (0.5, 1.0, 1.5 and 2.0 mm [perforated]). Assuming that the pitting holes are evenly distributed, the DOP is 6.25% (1/16), 12.5% (1/8), 25% (1/4) and 50% (1/2), respectively.

2.3 Simulation method

The quasi-static compression, low-speed impact and three-point bending were simulated by commercial ABAQUS nonlinear finite element software. The isotropic elastic–plastic constitutive model was adopted. Because the corrosion products of E690 steel were relatively loose and most of them would fall off (Zhao *et al.*, 2019), the mechanical properties of attached corrosion products could be ignored, thus the influence of corrosion products was not considered here. The material mechanical parameters are: density ρ_s 7850 kg/m^3, Young's modulus E_S 210 GPa, Poisson's ratio v 0.3 and yield strength σ_s 739 MPa. The model adopts von Mises yield criterion and J2 flow rule.

2.3.1 Quasi-static compression

The real stress–strain curve was used in the simulation without considering the strain rate effect. The lower pressure plate was fixed, and the upper pressure plate was compressed by 2 mm downward. The solid unit was used for calculation. Our previous results show (Liu, 2021) that uniform corrosion of the outer panel has little effect on quasi-static mechanical properties. Therefore, here we only consider the influence of pitting depths (0.5, 1.0, 1.5 and 2.0 mm) when DOP = 50%. For cores, different DOPs (6.25%, 12.5%, 25% and 50%) were considered apart from the pitting depths.

The area under the quasi-static compressive curve represents the energy absorption capacity of the panel. The total energy absorption (TEA) can be defined as W_v (Yan *et al.*, 2014):

$$\mathrm{W_v} = \int_0^{\overline{\varepsilon}} \sigma d\varepsilon \tag{3}$$

where σ, ε and $\overline{\varepsilon}$ are the compression stress, compression strain and the upper limit of strain integration of 0.5. Then the specific energy absorption (SEA) W_m can be obtained (Yan *et al.*, 2014):

$$\mathrm{W_m} = W_v/(\overline{\rho} * \rho_s) \tag{4}$$

where W_v is the TEA in equation (3), $\overline{\rho}$ is the relative density in equation (1) and ρ_s is the density of material.

2.3.2 Low-speed impact

The principle of free fall and Jaynes–Cummings model was adopted, and the dynamic parameter C is 0.021(Yang *et al.*, 2019). The lower pressure plate was fixed, and the upper pressure plate was compressed by 2 mm downward. The solid unit was used for simulation. Similar to quasi-static compression, the DOP = 50% with various corrosion depths of the upper panel was calculated for comparison. For cores,

Figure 1 Finite element simulation model of E690 steel panel

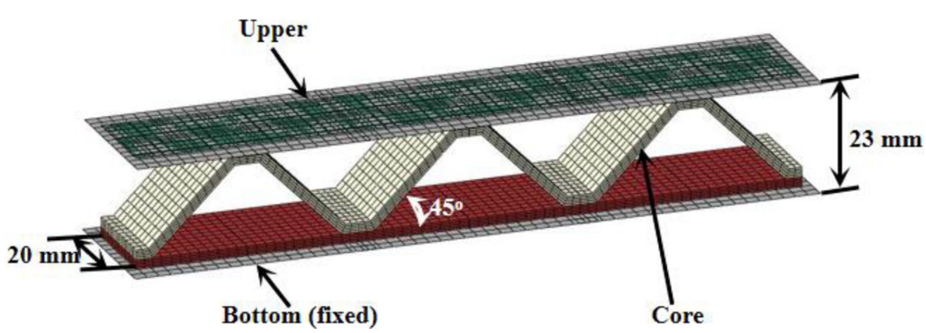

Figure 2 Quasi-static compression loading–displacement curves (a–e) and final failure morphologies (a_1–e_1) of E690 panel with different DOP and pitting depths

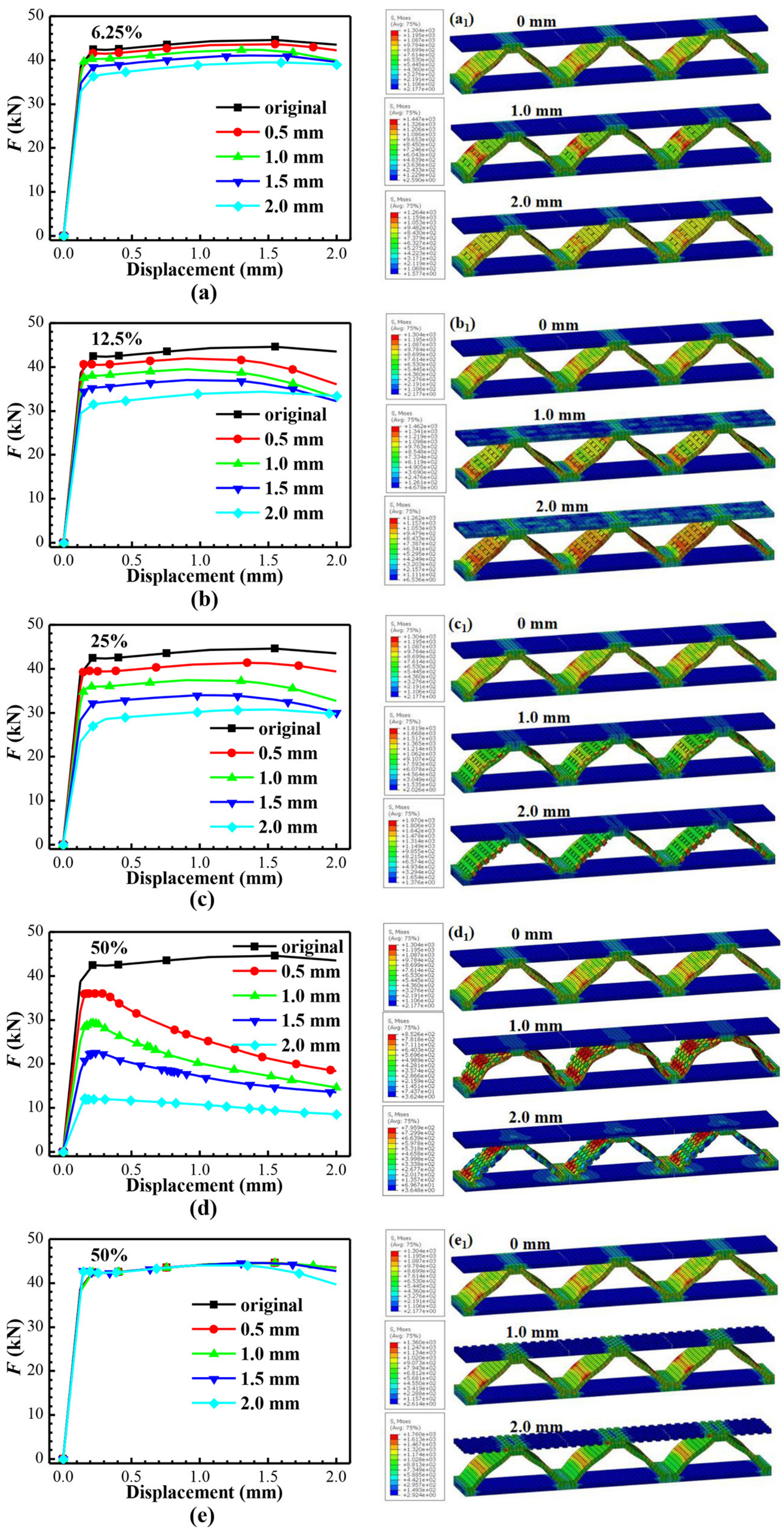

Note: core – 6.25% (a, a_1), core – 12.5% (b, b_1), core – 25% (c, c_1), core – 50% (d, d_1) and upper – 50% (e, e_1)

different DOPs (6.25%, 12.5%, 25% and 50%) and pitting depths (0.5, 1.0, 1.5 and 2.0 mm) were all considered.

2.3.3 Three-point bending

Considering the difficulty of three-point bending deformation, the shell body element was used for calculation. Here, the most severe pitting case was taken into account, that is, the pitting corrosion had led to the perforation of the structure, the corrosion depth was a fixed 2.0 mm and the change of DOPs (6.25%, 12.5%, 25% and 50%) on mechanical properties of the structure was simulated.

3. Results and discussion

3.1 Quasi-static compression

Figure 2 shows the stress–displacement curves (a–d) of quasi-static compression of E690 panel with different DOPs (6.25%, 12.5%, 25%, 50%) and corrosion depths (0.5, 1.0, 1.5 and 2.0 mm) and stress distribution (a_1–d_1) with corresponding displacement of 2 mm. For comparison, the quasi-static compression stress–displacement curves of upper panel with different pitting depths when DOP = 50% and the stress distribution images are also given in Figure 2(e and e_1). It can be seen that pitting depths of the upper panel have no obvious effect on the whole mechanical property of quasi-static compression and the curves are mostly overlapped. As can be seen from Figure 2(a)–(d), the peak load and SEA decrease with the increase of DOP and the pitting depth, indicating that the pitting could greatly deteriorate the mechanical properties of E690 panel.

The data in Figure 2 is analyzed and the results are listed in Table 1 and shown in Figure 3. It can be seen that the increase of pitting depth on upper panel will lead to a decrease in structure mass, but the strength, stiffness and peak load of the panel all decrease slightly, and the SEA increases rather than decreases, indicating that the pitting corrosion of the upper panel has no significant effect on the mechanical behavior of E690 panel under quasi-static compression condition. Here, we focus on the change of quasi-static mechanical properties of core after pitting corrosion. It can be seen from the data in Table 1 that the quasi-static mechanical properties decrease gradually with the increase of DOP. When the pitting depth is 2 mm, the mass of the sample with DOP = 50% is only 16% lower than that of without corrosion, but the stiffness, peak load and SEA is 74%, 72% and 71% lower. The influence of DOP is greater than that of pitting depth [see Figure 3(e) and (f)]. Thus, the DOP and pitting depth of core should be strictly controlled. Once the core is corroded, the deterioration of bearing capacity of the structure will be promoted.

3.2 Low-speed impact

Figure 4 displays the stress–displacement curves (a–d) of low-speed impact of E690 panel with different DOPs (6.25%, 12.5%, 25%, 50%) and corrosion depths (0.5, 1.0, 1.5 and 2.0 mm) and stress distribution (a_1–d_1) with corresponding displacement of 2 mm. The corresponding curves of upper panel with various pitting depths when DOP = 50% are also given in Figure 4(e and e_1). As with quasi-static compression, the pitting of the upper panel has no obvious effect on the mechanical property of low-speed impact. The peak load and SEA decrease with the increase of DOP and the pitting depth [see Figure 4(a)–(d)], which indicates that the pitting corrosion of core greatly worsens the mechanical properties of E690 panel.

Table 1 Mechanical properties of quasi-static compression of E690 panel with various DOPs (6.25%, 12.5%, 25%, 50%) and pitting depths (0.5, 1.0, 1.5 and 2.0 mm)

Corrosion part	DOP, (%)	Pit depth, (mm)	Mass, (g)	Strength, (N)	Stiffness, (N/mm)	Peak load, (N)	W_m, (J/g)
Core	Comparison	0	47.8	38,650.5	309,204.0	42,427.4	1,762.3
	6.25	0.5	47.5	37,783.3	302,266.4	41,557.9	1,733.4
		1.0	47.3	36,423.3	291,386.4	40,165.6	1,687.7
		1.5	47.0	34,792.3	278,338.4	38,479.4	1,643.4
		2.0	46.8	32,941.3	263,530.4	36,342.8	1,586.0
	12.5	0.5	47.3	37,105.6	296,844.8	40,763.9	1,654.4
		1.0	46.8	34,941.8	279,534.4	37,989.0	1,561.7
		1.5	46.3	32,490.6	259,924.8	35,054.4	1,493.1
		2.0	45.9	29,419.1	235,352.8	31,558.6	1,407.1
	25	0.5	46.8	35,843.9	286,751.2	39,624.0	1,666.9
		1.0	45.9	32,241.4	257,931.2	35,954.1	1,523.8
		1.5	44.9	28,251.2	226,009.6	32,169.3	1,409.5
		2.0	44.0	23,353.6	186,828.8	28,530.6	1,299.3
	50	0.5	45.9	32,017.1	25,6136.8	35,842.1	1,108.6
		1.0	44.0	25,238.5	20,1908.0	29,216.2	918.2
		1.5	42.1	18,114.3	14,4914.4	22,619.7	796.1
		2.0	40.2	9,896.8	79,174.1	11,999.2	503.9
Upper	50	0.5	46.0	38,376.2	307,009.6	42,429.7	1,830.8
		1	44.1	38,109.6	304,876.8	42,434.1	1,905.1
		1.5	42.3	37,702.8	301,622.4	42,817.2	1,985.4
		2	40.5	36,927.6	295,420.8	42,824.3	2,039.6

Figure 3 Mechanical properties of quasi-static compression of E690 panel with various DOPs (6.25%, 12.5%, 25%, 50%) and pitting depths (0.5, 1.0, 1.5 and 2.0 mm)

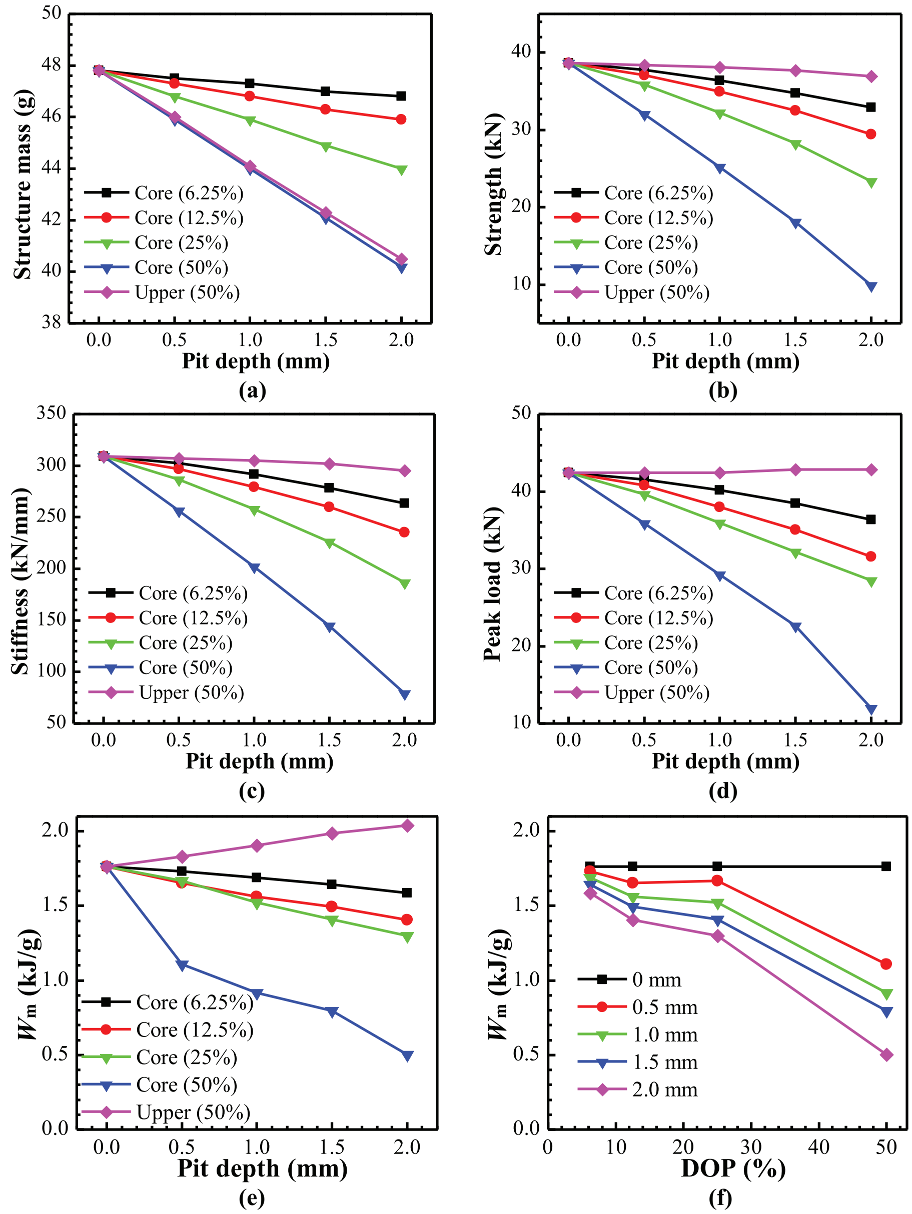

Notes: (a) Structure mass; (b) strength; (c) stiffness; (d) peak load; (e) SEA changes with pit depth; (f) SEA changes with DOP

The parsed data in Figure 4 is listed in Table 2 and shown in Figure 5. With the increase of the pitting depth on the upper panel when DOP = 50%, the pitting corrosion of panel will lead to a stable peak and an increase in SEA, indicating that the pitting corrosion of the upper panel has no significant effect on the mechanical behavior of E690 panel under low-speed impact condition. However, pitting corrosion has a greater influence on the core (see Table 2 and Figure 5), the low-speed impact mechanical properties (peak load and SEA) present the linear rule with the increase of pitting depth when the DOP is within 0–25% and the decreasing range increases with the increase of DOP; when the DOP increases to 50%, the linear law does not exist. When the pitting depth is 2 mm and DOP = 50%, the peak load and SEA decrease by 57% and 70%, respectively, compared with that of without pitting. To compare the factor the pitting corrosion depth and DOP, which has a greater impact on the bearing capacity of the core, a closer analysis of the data in Table 2 is conducted. It can be seen that under the same DOP, when the pitting corrosion increases from 0 to 2 mm, the peak load decreases to 16.5% (DOP = 6.25%), 26.4% (DOP = 12.5%), 33.5% (DOP = 12.5%) and 56.4% (DOP = 50%), respectively. Whereas, when the pitting depth is the same and

Figure 4 Low-speed impact loading–displacement curves (a–e) and final failure morphologies (a_1–e_1) of E690 panel with different DOPs (6.25%, 12.5%, 25%, 50%) and pitting depths (0.5, 1.0, 1.5 and 2.0 mm)

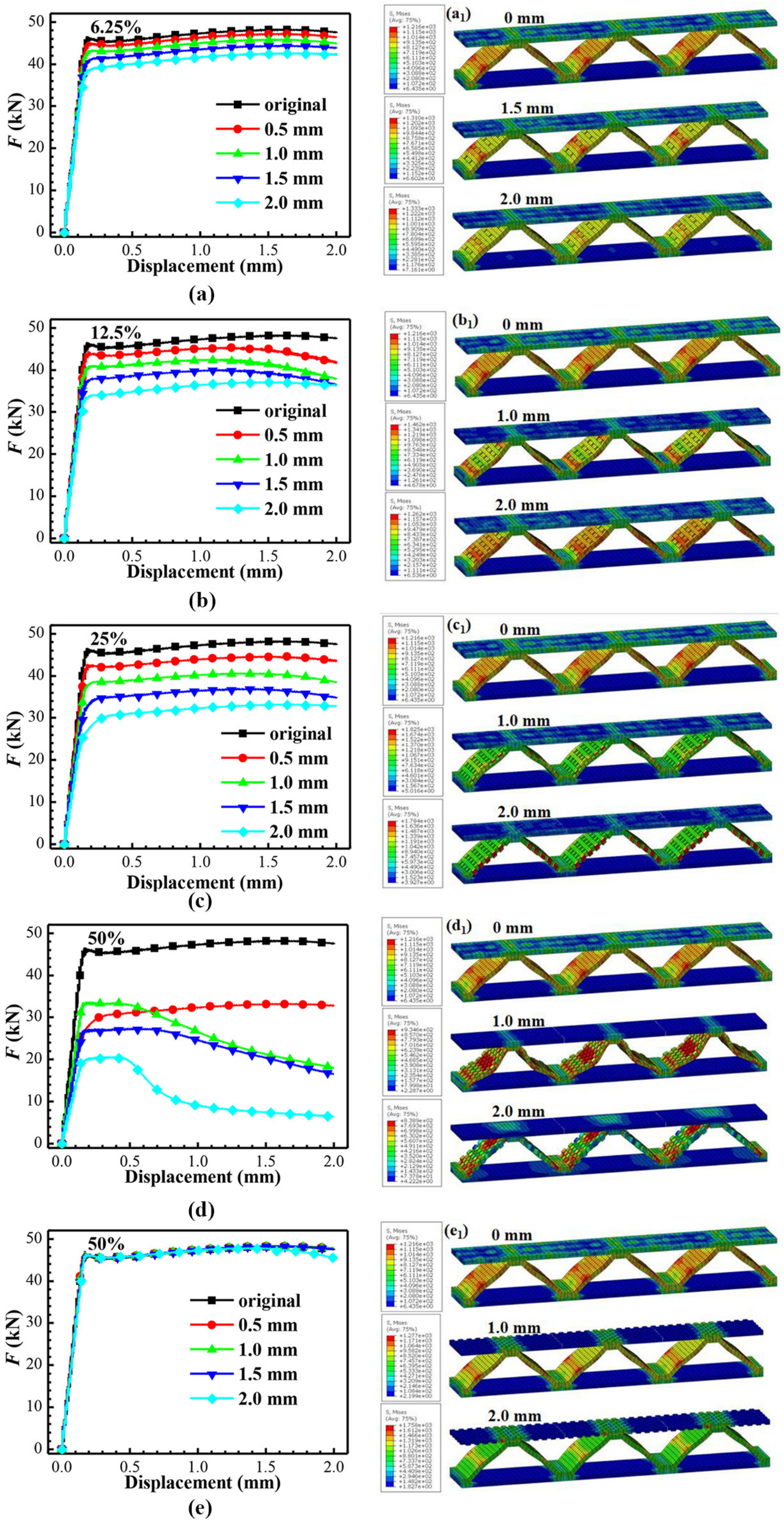

Note: core – 12.5% (b, b_1), core – 25% (c, c_1), core – 50% (d, d_1) and upper – 50% (e, e_1)

Anti-Corrosion Methods and Materials
Volume 69 · Number 4 · 2022 · 351–361

Table 2 Mechanical properties of low-speed impact of E690 panel with different DOPs (6.25%, 12.5%, 25%, 50%) and pitting depths (0.5, 1.0, 1.5 and 2.0 mm)

Corrosion part	DOP, (%)	Pit depth, (mm)	Mass, (g)	Peak load, (N)	W_m, (J/g)
Core	Comparison	0	47.8	46,121.8	1,894.1
	6.25	0.5	47.5	44,732.3	1,859.9
		1	47.3	43,017.1	1,820.1
		1.5	47.0	41,341.3	1,767.0
		2	46.8	38,518.3	1,696.8
	12.5	0.5	47.3	43,961.7	1,802.3
		1	46.8	40,845.7	1,695.2
		1.5	46.3	37,697.1	1,611.6
		2	45.9	33,913.1	1,505.9
	25	0.5	46.8	42,246.5	1,793.6
		1	45.9	38,539.1	1,660.8
		1.5	44.9	34,119.4	1,534.1
		2	44.0	30,684.4	1,392.7
	50	0.5	45.9	33,069.5	1,290.4
		1	44.0	30,416.8	1,150.8
		1.5	42.09	26,754.3	1,070.6
		2	40.21	20,053.5	559.2
Upper	50	0.5	45.95	45,894.3	1,964.0
		1	44.14	46,139.4	2,040.4
		1.5	42.34	45,955.2	2,131.1
		2	40.53	46,251.7	2,204.3

Figure 5 Mechanical properties of low-speed impact of E690 panel with different DOPs (6.25%, 12.5%, 25%, 50%) and pitting depths (0.5, 1.0, 1.5 and 2.0 mm)

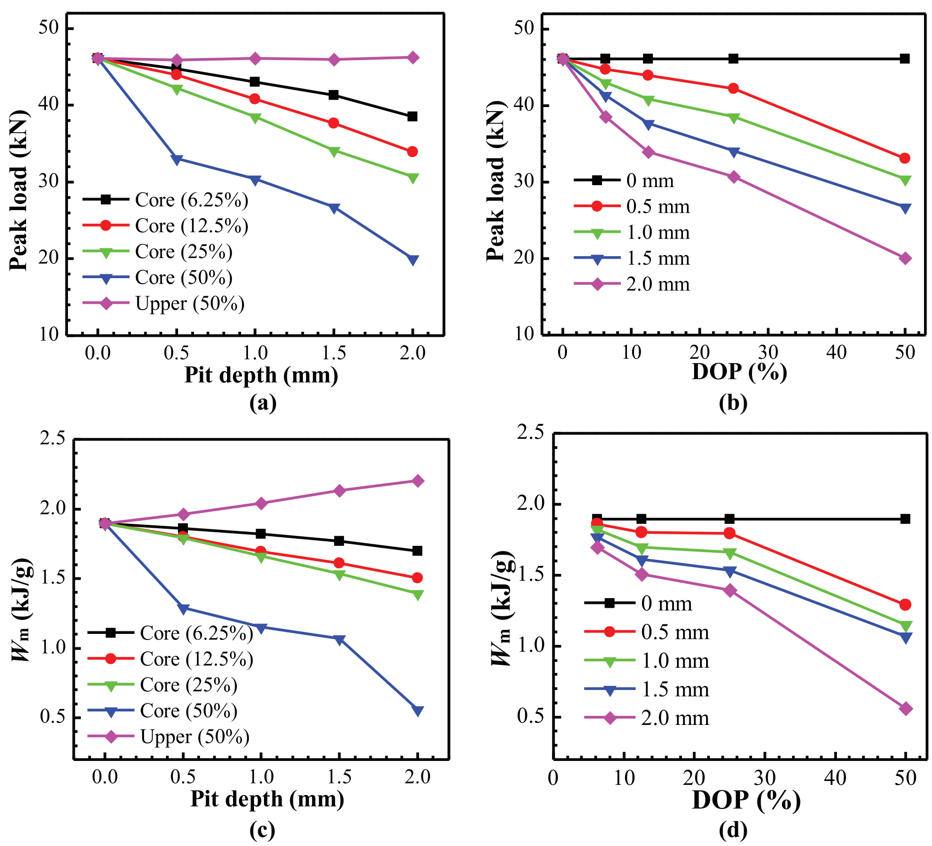

Notes: (a) Peak load changes with pit depth; (b) peak load changes with DOP; (c) SEA changes with pit depth; (d) SEA changes with DOP

DOP increases from 0 to 50%, the peak load decreases to 34.1%, 42.0% and 56.5% when the pitting depth is 0.5, 1, 1.5 and 2 mm, respectively. So it can be deduced that the influence of DOP is greater than that of pitting depth.

3.3 Three-point bending

Figure 6 shows the three-point bending stress displacement curves [see Figure 6(a)–(c)] of E690 panel with various DOPs (6.25%, 12.5%, 25%, 50%) after corrosion perforation (2 mm) and the corresponding stress distribution images [see Figure 6(a_1–c_1)] of panel after displacement of 10 mm. It can be seen that the mechanical properties of panel can be reduced by pitting corrosion with various DOPs, but the corroded mechanical properties of upper and bottom panel are better than that of core.

Figure 6 Three-point bending loading–displacement curves (a–c) and final failure morphology (a_1–c_1) of E690 panel with various DOPs (6.25%, 12.5%, 25%, 50%) with a fixed 2 mm pitting depth

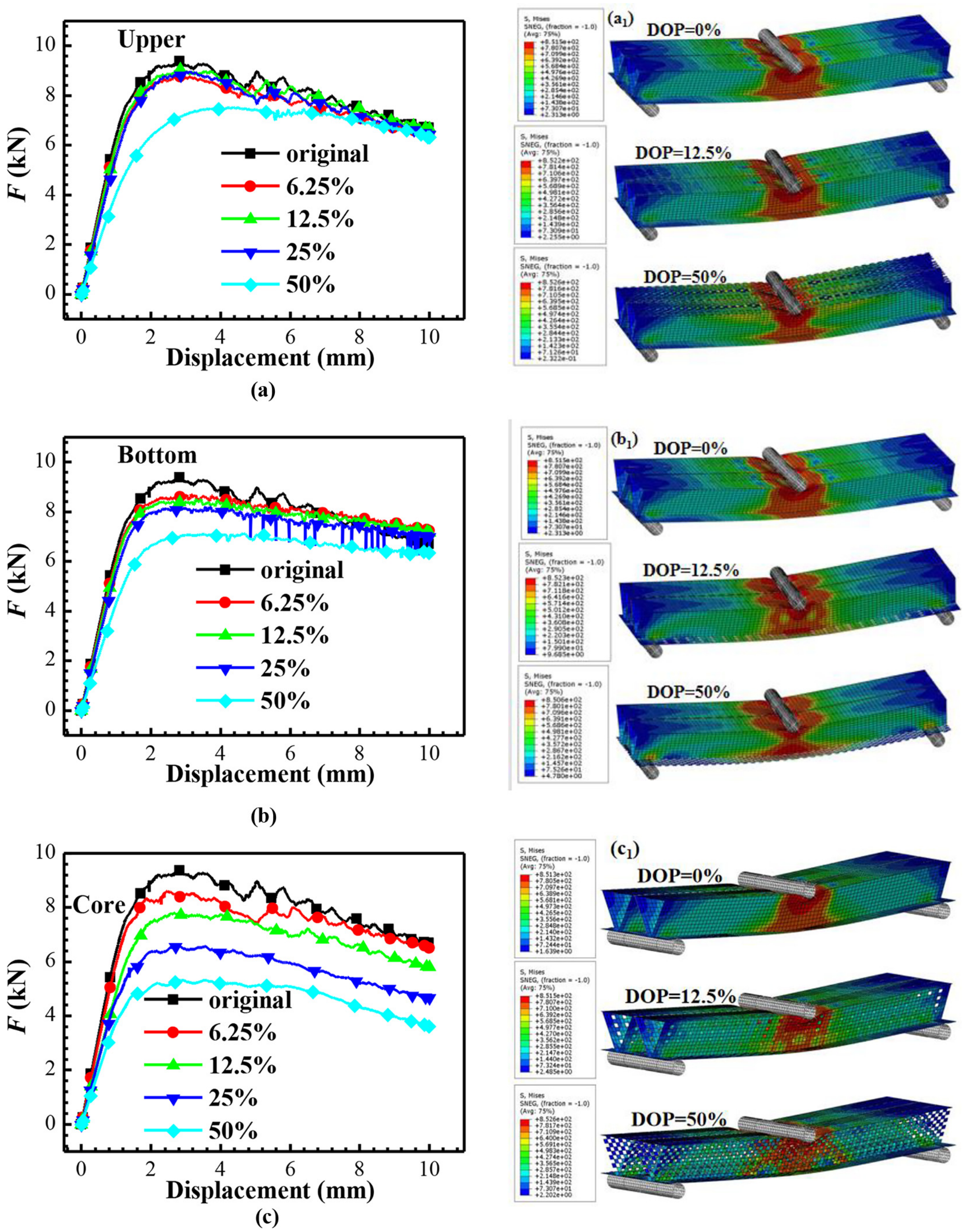

Note: upper (a, a_1), bottom (b, b_1) and core (c, c_1)

The analyzed results of three-point bending stress–displacement curves (Figure 6) are listed in Table 3 and shown in Figure 7. It can be seen that when the panel is perforated, the structure mass of the upper, bottom and core of the panel decreases linearly with the increase of DOP. The strength, stiffness, peak load and SEA of upper and bottom panel decrease slightly when the DOP is less than 25% and increase when DOP = 50%. The above mechanical parameters decrease rapidly when the DOP of core increases. When the DOP of core is 50%, the mass is only reduced by 20%, but the strength, stiffness, peak load and the SEA are 43%, 41%, 43% and 26% lower than that of original sample. Therefore, the DOP corrosion in the core of panel should be strictly controlled to prevent adverse effects on the mechanical properties of the structure.

4. Conclusions

- The quasi-static compression mechanical properties of E690 panel can be greatly reduced by the pitting corrosion of the core; however, the corrosion pits on the outer panel shows no evident effect. The mechanical properties of panel decrease with the increase of the pitting depth and DOP, and the influence of DOP shows more significant.

Figure 7 Mechanical properties of three-point bending of E690 panel with various DOP (6.25%, 12.5%, 25%, 50%) with a fixed 2 mm pitting depth

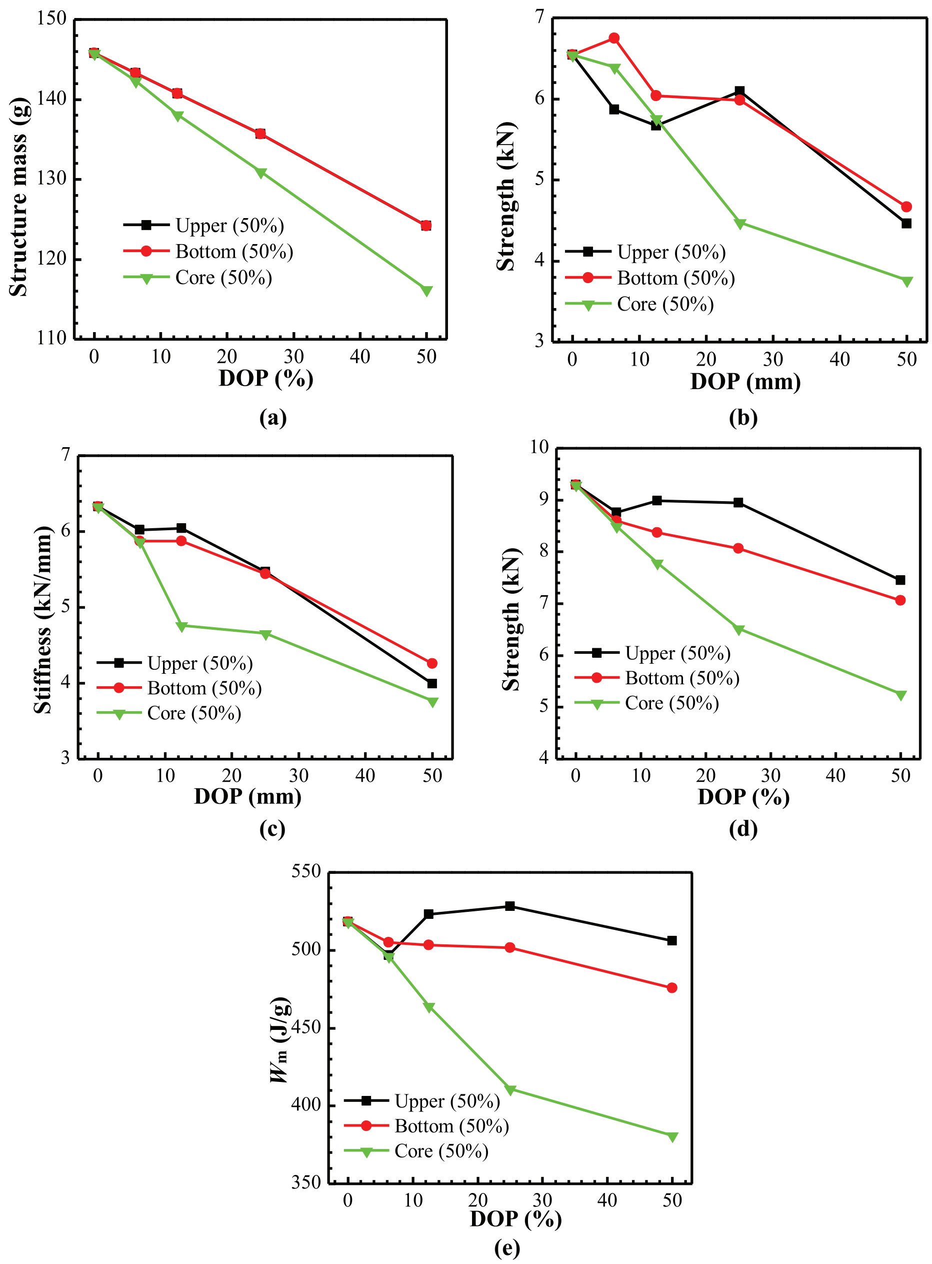

Notes: (a) Structure mass; (b) strength; (c) bending stiffness; (d) peak load; (e) SEA

Table 3 Mechanical properties of three-point bending of E690 panel with different DOP (6.25%, 12.5%, 25%, 50%) with a fix 2 mm pitting depth

Corrosion part	DOP, (%)	Mass, (g)	Strength, (,N)	Stiffness, (N/mm)	Peak load, (N)	W_m, (J/g)
Comparison	0	145.8	6,542.3	6,331.8	9,288.5	518.3
Upper	6.25	143.3	5,865.4	6,021.1	8,760.2	497.0
	12.50	140.7	5,665.9	6,042.3	8,981.8	523.0
	25	135.7	6,091.3	5,468.6	8,947.2	528.3
	50	124.2	4,460.0	3,993.4	7,450.9	505.9
Bottom	6.25	143.3	6,745.6	5,874.7	8,595.2	505.0
	12.50	140.7	6,039.1	5,874.0	8,372.1	503.2
	25	135.7	5,980.2	5,440.7	8,068.0	501.6
	50	124.2	4,668.4	4,261.7	7,066.4	475.8
Core	6.25	142.3	6,395.7	5,869.3	8,499.2	496.0
	12.5	138.1	5,758.4	4,759.0	7,788.9	464.3
	25	131.0	4,471.3	4,655.0	6,518.8	411.0
	50	116.2	3,761.8	3,767.1	5,255.4	381.0

- The pitting corrosion of outer panel has no obvious effect on the mechanical properties at low-speed impact. The peak load and SEA decrease linearly with the increase of corrosion depth when the DOP is small ($< 25\%$), and the decrease amplitude increases with the increase of DOP. The influence degree of DOP is greater than that of pitting depth.
- When the DOP of upper and bottom panel is less than 25%, the mechanical properties of three-point bending decrease slightly, but with the increase of the DOP in the core, the mechanical properties decrease rapidly. The mechanical property of panel decreases amplitude are larger than that of structure mass. Therefore, the pitting corrosion in the panel core should be strictly controlled to prevent adverse effects on the mechanical properties of the structure.

References

Anghel, C.I. (2009), "Risk assessment for pipelines with active defects based on artificial intelligence methods", *International Journal of Pressure Vessels and Piping*, Vol. 86 No. 7, pp. 403-411.

Bai, X.H., Zheng, Z.H. and Nakayama, A. (2019), "Heat transfer performance analysis on lattice core sandwich panel structures", *International Journal of Heat and Mass Transfer*, Vol. 143, p. 18525.

Chiodo, M. and Ruggieri, C. (2009), "Failure assessments of corroded pipelines with axial defects using stress-based criteria: numerical studies and verification analyses", *International Journal of Pressure Vessels and Piping*, Vol. 86 Nos 2/3, pp. 164-176.

Caleyo, F., Velazquez, J.C., Valor, A. and Hallen, J.M. (2009), "Probability distribution of pitting corrosion depth and rate in underground pipelines: a Monte Carlo study", *Corrosion Science*, Vol. 51 No. 9, pp. 1925-1934.

Chen, M., Pang, K., Liu, Z., Wu, J. and Li, X. (2018), "Influence of rust permeability on corrosion of E690 steel in industrial and non-industrial marine splash zones", *Journal of Materials Engineering & Performance*, Vol. 27 No. 7, pp. 1-8.

Deifalla, A. (2020), "Design of lightweight concrete slabs under two-way shear without shear reinforcements: a comparative study and a new formula", *Engineering Structures*, Vol. 222 No. 1, p. 111076.

Fu, Q., Fang, H., Wu, R.X., Yu, X.H. and Li, H.J. (2018), "A computational investigation of the group effect of pits on the ultimate strength of steel plates", *China Ocean Engineering*, Vol. 32 No. 6, pp. 665-674.

Han, L.H., Liu, M., Luo, S.J. and Lu, T.J. (2019), "Fatigue and corrosion fatigue behaviors of G105 and S135 high−strength drill pipe steels in air and H_2S environment", *Process Safety and Environmental Protection*, Vol. 124, pp. 63-74.

Kwon, K.Y. (2019), "Welding length estimation based on lightweight model for construction of offshore structures", *Transactions of the Korean Society of Mechanical Engineers - A*, Vol. 43 No. 2, pp. 111-118.

Kalinin, S.Y., Razumova, N.V. and Linkov, A.D. (2020), "Description of the information service for high-precision monitoring of the composite engineering structures' displacements and deformations to ensure the forecasting technological emergencies problems' solution", *IOP Conference Series: Materials Science and Engineering*, Vol. 913 No. 5, p. 52039.

Liu, M., Cheng, X.Q., Li, X.G. and Lu, T.J. (2017), "Corrosion behavior of low-Cr steel rebars in alkaline solutions with different pH in the presence of chlorides", *Journal of Electroanalytical Chemistry*, Vol. 803 No. 15, pp. 40-50.

Liu, M., Cheng, X.Q., Li, X.G., Pan, Y. and Li, J. (2016), "Corrosion behavior and durability of low-alloy steel rebars in marine environment", *Journal of Materials Engineering and Performance*, Vol. 25 No. 11, pp. 4967-4979.

Liu, Z.Y., Hao, W.K., Wu, W., Luo, H. and Li, X.G. (2019a), "Fundamental investigation of stress corrosion cracking of E690 steel in simulated marine thin electrolyte layer", *Corrosion Science*, Vol. 148, pp. 388-396.

Liu, M., Luo, S.J., Shen, Y. and Lin, X.Z. (2019b), "Corrosion fatigue crack propagation behavior of S135 high–strength drill pipe steel in H_2S environment", *Engineering Failure Analysis*, Vol. 97, pp. 493-505.

Liu, M. (2021), "Effect of uniform corrosion on mechanical behavior of E690 high-strength steel lattice corrugated panel in marine environment: a finite element analysis", *Materials Research Express*, Vol. 8 No. 6, p. 066510.

Nakai, T., Matsushita, H. and Yamamoto, N. (2006), "Effect of pitting corrosion on the ultimate strength of steel plates subjected to in-plane compression and bending", *Journal of Marine Science and Technology*, Vol. 11 No. 1, pp. 52-64.

Panda, H.S. and Jagadeesha, T. (2021), "Impact analysis of rifle bullet on corrugated sandwich panel structures for defense applications", *Materials Today: Proceedings*, Vol. 46 No. 17, pp. 8444-8449.

Rahbar-Ranji, A., Niamir, N. and Zarookian, A. (2015), "Ultimate strength of stiffened plates with pitting corrosion", *International Journal of Naval Architecture and Ocean Engineering*, Vol. 7 No. 3, pp. 509-525.

Rabiee, A. and Ghasemnejad, H. (2019), "Lightweight design to improve crushing behaviour of multi-stitched composite tubular structures under impact loading", *Thin-Walled Structures*, Vol. 135, pp. 109-122.

Said, H., Abdelouahed, L., Abdelhadi, E. and Zitouni, A. (2015), "Calculation of defects in pressurised cylindrical shells instrumented by acoustic emission and strain gauges", *Materiaux & Techniques*, Vol. 103 No. 7, p. 702.

Saad-Eldeen, S., Garbatov, Y. and Soares, C.G. (2013), "Effect of corrosion severity on the ultimate strength of a steel box girder", *Engineering Structures*, Vol. 49, pp. 560-571.

Turnbull, A., Mccartney, L.N. and Zhou, S. (2006), "A model to predict the evolution of pitting corrosion and the pit-to-crack transition incorporating statistically distributed input parameters", *Corrosion Science*, Vol. 48 No. 8, pp. 2084-2105.

Wang, X., Li, X., Yue, Z.S., Yu, R.P., Zhang, Q.C., Du, S.F., Yang, Z.K., Han, B. and Lu, T.J. (2020), "Optimal design of metallic corrugated sandwich panels with polyurea-metal laminate face sheets for simultaneous vibration attenuation and structural stiffness", *Composite Structures*, Vol. 256, p. 112994.

Yan, L.L., Yu, B., Han, B., Chen, C.Q., Zhang, Q.C. and Lu, T.J. (2013), "Compressive strength and energy absorption of sandwich panels with aluminum foam-filled corrugated cores", *Composites Science and Technology*, Vol. 86 No. 7, pp. 142-148.

Yan, L.L., Yu, B., Han, B., Chen, C.Q., Zhang, Q.C. and Lu, T.J. (2014), "Three-point bending of sandwich beams with aluminum foam-filled corrugated cores", *Materials & Design*, Vol. 60, pp. 510-519.

Yang, X.Q., Yang, H. and Zhang, S.M. (2019), "Rate-dependent constitutive models of S690 high-strength structural steel", *Construction and Building Materials*, Vol. 198, pp. 597-607.

Zhao, T., Liu, Z.Y., Xu, X.X., Li, Y., Du, C.W. and Liu, X.G. (2019), "Interaction between hydrogen and cyclic stress and its role in fatigue damage mechanism", *Corrosion Science*, Vol. 157, pp. 146-156.

Corresponding author

Ming Liu can be contacted at: liuming0313@xjtu.edu.cn